
E-Valuating Classifier Two-Sample Tests

Teodora Pandeva
AI4Science Lab, AMLab
Informatics Institute
University of Amsterdam

Tim Bakker
AMLab
Informatics Institute
University of Amsterdam

Christian A. Naesseth
AMLab
Informatics Institute
University of Amsterdam

Patrick Forré
AI4Science Lab, AMLab
Informatics Institute
University of Amsterdam

Abstract

We propose E-C2ST, a classifier two-sample test for high-dimensional data based on E-values. Compared to p -values-based tests, tests with E-values have finite sample guarantees for the type I error. E-C2ST combines ideas from existing work on split likelihood ratio tests and predictive independence testing. The resulting E-values incorporate information about the alternative hypothesis. We demonstrate the utility of E-C2ST on simulated and real-life data. In all experiments, we observe that when going from small to large sample sizes, as expected, E-C2ST starts with lower power compared to other methods but eventually converges towards one. Simultaneously, E-C2ST's type I error stays substantially below the chosen significance level, which is not always the case for the baseline methods. Finally, we use an MRI dataset to demonstrate that multiplying E-values from multiple independently conducted studies leads to a combined E-value that retains the finite sample type I error guarantees while increasing the power.

1 Introduction

Statistical hypothesis testing is an essential tool in evidence-based research. An example from medicine is a randomized controlled trial (RCT) experiment where we test whether a treatment has no effect on patients (null hypothesis) versus a positive one (alternative hypothesis). Ideally, we would like the statistical test to reject an ineffective treatment with a high probability, i.e., to keep the probability of falsely rejecting the null hypothesis, called *type I error*, low. This is usually controlled by a decision boundary, called *significance level*, denoted by α . We reject the null hypothesis if the computed p -value is below α . Thus, the type I error becomes upper-bounded by the significance level. The choice of α is crucial not only for the type I error, but also for the *type II error*, which

refers to the probability of failing to reject the null when the alternative hypothesis is true. A low α leads to a low type I error. Unfortunately, lower α also leads to increasing type II error, or, equivalently, decreasing *power* (defined as $1 - \text{type II error}$). We refer to this trade-off as detection error trade-off. Therefore, the choice of α is often a subject of debate in the scientific community [BBJ⁺18].

In this work, we consider classifier two-sample tests, which try to answer the statistical question of whether two populations obtained independently are statistically significantly different. Proposed solutions to the problem have been focusing on developing tests with high power to distinguish real from generated data [LPO16], noise from data [LPO16, HTF01, GH12, MSC⁺13, GPAM⁺14] and are widely used in simulation-based inference [LBG⁺21]. However, due to the type I and type II error trade-off discussed above, these tests might not be suitable in some applications, e.g., the aforementioned RCT example. To address this issue, we will introduce classifier two-sample tests with guaranteed type I error control lower than the significance level.

Two-sample testing procedures include classical approaches such as Student's and Welch's t-tests [Stu08, Wel47] comparing the means of two normally distributed samples; non-parametric tests, such as the Wilcoxon-Mann-Whitney test [MW47] that compare the ranks of the two populations in the combined datasets, or the Kolmogorov-Smirnov tests [Kol33, Smi39] and the Kuiper test [Kui60]. In the high-dimensional data regime, kernel methods [SS98] have been proposed, which compare the kernel embeddings of both populations [GBR⁺12, CRS15, JSCG16]. However, all these statistical two-sample tests become less powerful on more complex data such as images, text, etc. For that reason, deep learning extensions of the two sample tests have been developed, such as [LPO16, CC19, KKKL20, LXL⁺20], where one trains a model to distinguish the two populations on train data and conduct the statistical test on a test set. All listed methods estimate a p -value either via asymptotically valid approximations or via permutation methods. Based on such a p -value, one decides whether or not to reject the null with

significance α , historically chosen to be $\alpha = 0.05$.

Compared to p -values, E-variables have a finite sample type I error which is often lower than the chosen significance level. More formally, E-variables are simply non-negative variables E that satisfy

$$\text{for all } P \in \mathcal{H}_0 : \mathbb{E}_P[E] \leq 1,$$

i.e. the expectation of E with respect to any distribution from the null hypothesis distribution class \mathcal{H}_0 is less than one. An example of E-variables for singleton hypothesis classes are Bayes factors, i.e. we test if the unknown probability density p equals p_0 or p_A :

$$H_0 : p = p_0 \quad \text{vs.} \quad H_A : p = p_A.$$

Here, we assume that both hypotheses occur with equal probability. Then the Bayes factor given by $E(x) := \frac{p_A(x)}{p_0(x)}$ is an E-variable w.r.t. \mathcal{H}_0 since $\mathbb{E}_{p_0}[E] = \int \frac{p_A(x)}{p_0(x)} p_0(x) dx = 1 \leq 1$. Note that observing a very large value of E , which we call an E-value, provides evidence against the null hypothesis. The origin and interpretation of E-variables can be traced back to the work of [Jr56] in the context of gambling. Recently E-values have been reintroduced in the work of [GdHK20, Sha19] interpreted as bets against the null hypothesis.

We propose a classifier two-sample test based on E-values, called E-C2ST. First, we introduce the more general framework of *conditional* E-variables with their corresponding properties in Section 2.2. Then, in Section 3, we show how to construct E-variables by employing the *split-likelihood testing* procedure by [WRB20] for any null hypothesis. Afterward, we consider the special case of conditional independence testing. By combining the ideas developed in Section 3 and the existing work on predictive conditional independence testing framework by [BK17], we derive the corresponding E-values (see Section 4). In Section 5, we introduce our proposed classifier two-sample test based on E-variables, called E-C2ST, which formally derives from the proposed predictive conditional independence testing framework from Section 4. Finally, we compare E-C2ST experimentally to existing commonly used two-sample tests on simulated and more complex image data. We also simulate a meta-analysis study on MRI data and illustrate how E-variables can be easily utilized for combining independent studies. We explore the aforementioned type-I–type-II error trade-off by simultaneously tracking the change of type I and type II errors with increasing sample size.

Our empirical results show that even though E-C2ST has lower power than other methods, its power converges to 1 when the sample size is large enough. Furthermore, it always keeps the type I error substantially below the threshold level, which is not always the case for the baseline methods.

Our **contributions** can be summarized as follows

1. We formalize predictive conditional independence testing by means of E-variables.
2. Leveraging predictive independence testing allows us to develop an E-variable-based classifier two-sample test that has finite sample type I error guarantee.
3. By considering the type-I–type-II error trade-off of statistical tests, we compare E-C2ST to existing baseline methods. We show experimentally that it has a power that converges to one with increasing sample size while retaining type I error lower than the chosen significance level.

2 Hypothesis Testing with E-Variables

2.1 Hypothesis Testing

Consider a sample of data points $\mathcal{D} = \{x_1, \dots, x_N\}$ ¹, reflecting realizations of random variables X_1, \dots, X_N drawn from an unknown probability distribution $P \in \mathcal{P}(\Omega)$ coming from some unknown sample space Ω , where $\mathcal{P}(\Omega)$ is the set of all probability measures on Ω . In hypothesis testing, we usually consider two model classes:

$$\begin{aligned} \mathcal{H}_0 &= \{P_\theta \in \mathcal{P}(\Omega) \mid \theta \in \Theta_0\} & (\text{null hypothesis}), \\ \mathcal{H}_A &= \{P_\theta \in \mathcal{P}(\Omega) \mid \theta \in \Theta_A\} & (\text{alternative}), \end{aligned}$$

and we want to decide if P comes from \mathcal{H}_0 or from \mathcal{H}_A :

$$H_0 : P \in \mathcal{H}_0 \quad \text{vs.} \quad H_A : P \in \mathcal{H}_A,$$

based on the value of some test statistic $T^{(N)} = T(X_1, \dots, X_N)$. In most cases the data points come from the same space \mathcal{X} and we would at most observe countably many of such data points X_n . In this setting we can w.l.o.g. assume that $\Omega = \mathcal{X}^{\mathbb{N}}$. If we, furthermore, assume that the $X_n, n \in \mathbb{N}$, are drawn i.i.d. from P then $P((X_n)_{n \in \mathbb{N}}) = \bigotimes_{n=1}^{\infty} P(X_n)$ and we can directly incorporate the product structure into \mathcal{H}_0 and \mathcal{H}_A and restrict ourselves to one of those factors to state \mathcal{H}_i and (by slight abuse of notations) re-write for $i = 0, A$:

$$\mathcal{H}_i = \{P_\theta \in \mathcal{P}(\mathcal{X}) \mid \theta \in \Theta_i\}, \quad (1)$$

and implicitly assume that $P_\theta((X_n)_{n \in \mathbb{N}}) = \bigotimes_{n=1}^{\infty} P_\theta(X_n)$. Moreover, assume that our probability measures $P_\theta \in \mathcal{H}_i$, are given via a density w.r.t. a product reference measure μ . We will denote the density by $p_\theta(x)$ or $p(x|\theta)$, interchangeably.

¹In the following we will write small x if we either mean the realization of a random variable X or the argument of a function living on the same space. We use capital X for a data point if we want to stress its role as a random variable.

2.2 Conditional E-Variables

Now consider the more general *relative* framework where we allow hypothesis classes to come from a set of Markov kernels, which can be used to model *conditional* probability distributions:

$$\mathcal{H}_i = \{P_\theta : \mathcal{Z} \rightarrow \mathcal{P}(\mathcal{X}) \mid \theta \in \Theta_i\} \subseteq \mathcal{P}(\mathcal{X})^{\mathcal{Z}}, \quad (2)$$

where the latter denotes the space of all Markov kernels from \mathcal{Z} to \mathcal{X} , i.e. for each $P_\theta \in \mathcal{H}_i$ for fixed $z \in \mathcal{Z}$ $P_\theta(\cdot|z)$ is a valid probability measure on \mathcal{X} . An example of conditional hypothesis classes is given in Section 4, where the null hypothesis class represent the set of distributions that reflect the conditional independence of two variables after observing a third one.

With respect to \mathcal{H}_0 as defined in Equation 2 we can define corresponding E-variables which we call *conditional E-variables*²:

Definition 2.1 (Conditional E-variable). A conditional E-variable w.r.t. $\mathcal{H}_0 \subseteq \mathcal{P}(\mathcal{X})^{\mathcal{Z}}$ is a non-negative measurable map:

$$E : \mathcal{X} \times \mathcal{Z} \rightarrow \mathbb{R}_{\geq 0}, \quad (x, z) \mapsto E(x|z),$$

such that for all $P_\theta \in \mathcal{H}_0$ and $z \in \mathcal{Z}$ we have:

$$\mathbb{E}_\theta[E|z] := \int E(x|z) P_\theta(dx|z) \leq 1.$$

In Section 3, we will show that the M -split likelihood ratio test statistic [WRB20] can be written as a product of conditional E-variables, where in the above definition $\mathcal{Z} = \mathcal{X}^{n-1}$, the space from which previous data points were drawn.

One of the notable features of E-variables is their preservation under multiplication. We can easily combine (conditionally) independent E-variables by simply multiplying them which results in a proper E-variable. This property makes E-variables appealing for meta-analysis studies [GdHK20, VW21] as we will demonstrate later experimentally. A more general result states that we can combine backwards dependent conditional E-variables via multiplication which is formally given in the following Lemma:

Lemma 2.2 (Products of conditional E-variables). If $E^{(1)}$ is a conditional E-variable w.r.t. $\mathcal{H}_0^{(1)} \subseteq \mathcal{P}(\mathcal{Y})^{\mathcal{Z}}$ and $E^{(2)}$ a conditional E-variable w.r.t. $\mathcal{H}_0^{(2)} \subseteq \mathcal{P}(\mathcal{X})^{\mathcal{Y} \times \mathcal{Z}}$ then $E^{(3)}$ defined via their product:

$$E^{(3)}(x, y|z) := E^{(2)}(x|y, z) \cdot E^{(1)}(y|z),$$

²A formal definition of the "unconditional" E-variables introduced in Section 1 can be easily derived from Definition 2.1 by dropping \mathcal{Z} . Moreover, if E is an E-variable and $x \in \mathcal{X}$ a fixed point then we call $E(x)$ the E-value of x w.r.t. E .

is a conditional E-variable w.r.t.:

$$\mathcal{H}_0^{(3)} := \mathcal{H}_0^{(2)} \otimes \mathcal{H}_0^{(1)} \subseteq \mathcal{P}(\mathcal{X} \times \mathcal{Y})^{\mathcal{Z}},$$

where we define the product hypothesis as:

$$\mathcal{H}_0^{(2)} \otimes \mathcal{H}_0^{(1)} := \left\{ P_\theta \otimes P_\psi \mid P_\theta \in \mathcal{H}_0^{(2)}, P_\psi \in \mathcal{H}_0^{(1)} \right\},$$

with the product Markov kernels given by:

$$(P_\theta \otimes P_\psi)(dx, dy|z) := P_\theta(dx|y, z) P_\psi(dy|z).$$

2.3 Hypothesis Testing with Conditional E-Variables

In the context of statistical testing, we can evaluate an E-variable E on the given data points w.r.t. random variables X_1, \dots, X_N . Then the decision rule for rejecting the null hypothesis at significance level $\alpha \in [0, 1]$ becomes:

Reject \mathcal{H}_0 in favor of \mathcal{H}_A if $E(X_1, \dots, X_N) \geq \alpha^{-1}$.

Lemma 2.3 tells us that with this rule the type I error, the error rate of falsely rejecting the \mathcal{H}_0 , is bounded by α .

Lemma 2.3 (Type I error control). Let E be a conditional E-variable w.r.t. $\mathcal{H}_0 \subseteq \mathcal{P}(\mathcal{X})^{\mathcal{Z}}$. Then for every $\alpha \in [0, 1]$, $P_\theta \in \mathcal{H}_0$ and $z \in \mathcal{Z}$ we have:

$$P_\theta(E \geq \alpha^{-1}|z) \leq \alpha.$$

Proof. This follows from the Markov inequality:

$$P_\theta(E \geq \alpha^{-1}|z) \leq \frac{\mathbb{E}_\theta[E|z]}{\alpha^{-1}} \leq \frac{1}{\alpha^{-1}} = \alpha. \quad \square$$

Thus, the E-values can be transformed into more conservative p -values via the relation $p = \min\{1, 1/E\}$ such that for $P_\theta \in \mathcal{H}_0$ it holds $P_\theta(p \leq \alpha|z) \leq \alpha$. Note that a valid way of constructing an E-variable from the random variables X_1, \dots, X_N w.r.t. the observed sample points according to Lemma 2.2 is $E(X_1, \dots, X_N) = \prod_{i=1}^N E(X_i)$.

Remark 2.4 (Type II error and power). Justified by the law of large numbers, E-variables with $\mathbb{E}_P[\log E] > 0$ for $P \in \mathcal{H}_A$ have asymptotic power, at least in the i.i.d. case, because then:

$$\log E(X_1, \dots, X_N) = \sum_{n=1}^N \log E(X_n) \approx N \cdot \mathbb{E}_P[\log E].$$

However, providing a proper analysis in the more general, non-i.i.d. setting is out of the scope of this paper. In the appendix we provide a finite sample bound for the type II error, but (only) in the special case of (conditional) i.i.d. E-variables, which is based on Sanov's theorem, see Thm. A.1, [Csi84, Bal20]. Nonetheless, to deal with the general case, in the following section 3 we use the M -split likelihood ratio construction of E-variables from [WRB20], where we can optimize the power of the test by training the E-variables on some form of training set.

3 M -Split Likelihood Ratio Test

In general, constructing an E-variable with respect to any \mathcal{H}_0 is not a straightforward task. There exist two main approaches. The first approach, see [GdHK20], is based on the reverse information projection of the hypothesis space \mathcal{H}_A onto \mathcal{H}_0 . It is not data-dependent and can be shown to be growth-optimal in the worst case. However, the reverse information projection is not very explicit in general settings, especially when working with non-convex hypotheses, \mathcal{H}_A and \mathcal{H}_0 . The second approach is based on the split likelihood ratio test from [WRB20], which we will discuss in this section. Compared to the previous approach, this method yields a data-driven E-variable, which can in certain cases even be stated in closed form.

Assume that our data set $\mathcal{D} = \{X_1, \dots, X_N\}$ is of size N . We now split the index set $[N] := \{1, \dots, N\}$ into $M \geq 2$ disjoint batches:

$$[N] = \mathcal{I}^{(1)} \dot{\cup} \dots \dot{\cup} \mathcal{I}^{(M)}.$$

For $m = 1, \dots, M$ we also abbreviate:

$$\begin{aligned} \mathcal{I}^{(<m)} &:= \mathcal{I}^{(1)} \dot{\cup} \dots \dot{\cup} \mathcal{I}^{(m-1)}, \\ x^{(m)} &:= (x_n)_{n \in \mathcal{I}^{(m)}} \in \prod_{n \in \mathcal{I}^{(m)}} \mathcal{X} =: \mathcal{X}^{(m)}. \end{aligned}$$

and $x^{(<m)}, x^{(\leq m)}, \mathcal{I}^{(\leq m)}$, analogously.

Then for $m = 1, \dots, M$ we follow these steps:

1. Train a model on Θ_A on all previous points $x^{(<m)}$ in an arbitrary way (MLE, MAP, full Bayesian, etc.) and get $p_A(x|x^{(<m)})$. To achieve a high power of the test, the density $p_A(x|x^{(<m)})$ should reflect the true distribution in the best possible way to generalize well to unseen data.
2. Train a model on Θ_0 on the data points of the current batch $x^{(m)}$ (conditioned on the previous ones $x^{(<m)}$) via maximum-likelihood fitting (MLE):

$$\hat{\theta}_0^{(\leq m)} := \hat{\theta}_0^{(m)}(x^{(\leq m)}) := \operatorname{argmax}_{\theta \in \Theta_0} p_\theta(x^{(m)}|x^{(<m)}),$$

and get: $p_0(x|x^{(\leq m)}) := p(x|x^{(<m)}, \hat{\theta}_0^{(m)}(x^{(\leq m)}))$. Note that under i.i.d. assumptions there is no dependence on $x^{(<m)}$.

3. Evaluate both models on the current points $x^{(m)}$ and define $E^{(m)}$ via their ratio:

$$\begin{aligned} E^{(m)}(x^{(m)}|x^{(<m)}) &:= \frac{p_A(x^{(m)}|x^{(<m)})}{p_0(x^{(m)}|x^{(\leq m)})}, \\ &= \frac{p_A(x^{(m)}|x^{(<m)})}{\max_{\theta \in \Theta_0} p_\theta(x^{(m)}|x^{(<m)})}. \end{aligned} \quad (3)$$

Then $E^{(m)}$ constitutes a conditional E-variable, conditioned on the space $\mathcal{X}^{(<m)}$, w.r.t. $\mathcal{H}_0^{(m)}|^{(<m)}$.

For a fixed m , the m -th conditional E-variable is more doubtful against the alternative hypothesis class since it compares the \mathcal{H}_A -model's *test* performance, which is trained on $x^{(<m)}$, tested on $x^{(m)}$, with the \mathcal{H}_0 -model's *train* performance both trained and tested on the same $x^{(m)}$ in the i.i.d. case. This means that if the alternative is true, then the \mathcal{H}_A -model p_A has to perform better on $x^{(m)}$ than the \mathcal{H}_0 -model p_0 , while the latter was allowed to be directly (over)fitted on $x^{(m)}$. This heuristic intuition behind the m -th conditional E-variable explains why one would expect to need more samples to gather enough evidence for rejecting the null hypothesis \mathcal{H}_0 in favor of the alternative \mathcal{H}_A when testing with such E-variables in contrast to other tests.

It then follows from Lemma 2.2 that the product:

$$E := E^{(\leq M)} := \prod_{m=1}^M E^{(m)},$$

defines an E-variable w.r.t. $\mathcal{H}_0 = \mathcal{H}_0^{(\leq M)}$.

The M -split likelihood ratio test, for significance level $\alpha \in [0, 1]$, rejects the null hypothesis \mathcal{H}_0 if $E(X_1, \dots, X_N) \geq \alpha^{-1}$. Lemma 2.3 ensures that the type I error is bounded by α .

Remark 3.1 (Initialization and validation set). *In point 1. of the above test procedure, we emphasized that the power of the proposed test depends on the test performance of the predictive distributions $p_A(x|x^{(<m)})$. We can apply any well-known training technique to achieve high predictive performance, without violating the any of the properties of E-variables. For example, after we split the data into M partitions, for each of the $M - 1$ training procedures, we can further split the $x^{(<m)}$ dataset into train and validation set and use early stopping to prevent overfitting or even K -fold cross-validation for hyper-parameter tuning. Note that the test set $x^{(m)}$ does not participate in the training procedure.*

4 Predictive Conditional Independence Testing

In this section, we combine the ideas of predictive conditional independence testing from [BK17] with E-variables from the M -split likelihood ratio test from Section 3 based on [WRB20] to derive a proper E-variable for *conditional* independence testing. The desired two sample test will later on be reformulated as an independence test by utilizing the theoretical results discussed in this section.

As a reminder, in conditional independence testing we want to test if a random variable X is independent, or not, of Y conditioned on Z :

$$H_0 : X \perp\!\!\!\perp Y \mid Z \quad \text{vs.} \quad H_A : X \not\perp\!\!\!\perp Y \mid Z,$$

based on data $\mathcal{D} = \{(X_1, Y_1, Z_1), \dots, (X_N, Y_N, Z_N)\}$. The corresponding (*full*) hypothesis spaces, in the i.i.d. setting, are:

$$\begin{aligned}\mathcal{H}_0^{\text{fl}} &= \{P_\theta(X|Z) \otimes P_\theta(Y|Z) \otimes P_\theta(Z) \mid \theta \in \Theta_0\}, \\ \mathcal{H}_A^{\text{fl}} &= \{P_\theta(X, Y, Z) \mid \theta \in \Theta_A\} \setminus \mathcal{H}_0.\end{aligned}$$

If we assume that $P(X, Z)$ is *fixed* for \mathcal{H}_0 and \mathcal{H}_A then this simplifies to the following product hypothesis classes, $i = 0, A$:

$$\mathcal{H}_i^{\text{fx}} := \mathcal{H}_i^{\text{pd}} \otimes \{P(X, Z)\}, \quad (4)$$

where the conditional hypothesis classes $\mathcal{H}_i^{\text{pd}} \subseteq \mathcal{P}(\mathcal{Y})^{\mathcal{X} \times \mathcal{Z}}$ of *predictive distributions* are given by:

$$\begin{aligned}\mathcal{H}_0^{\text{pd}} &= \{P_\theta(Y|Z) \mid \theta \in \Theta_0\}, \\ \mathcal{H}_A^{\text{pd}} &= \{P_\theta(Y|X, Z) \mid \theta \in \Theta_A\} \setminus \mathcal{H}_0.\end{aligned} \quad (5)$$

Equation 3 applied to $\mathcal{H}_i^{\text{fx}}$ under i.i.d. assumptions leads us to the following m -th conditional E-variable, using the abbreviation $w = (x, y, z)$:

$$E^{(m)}(w^{(m)} | w^{(<m)}) = \frac{p_A(y^{(m)} | x^{(m)}, z^{(m)}, w^{(<m)})}{p(y^{(m)} | z^{(m)}, \hat{\theta}_0(y^{(m)}, z^{(m)}))}. \quad (6)$$

The reason that we applied Equation 3 to $\mathcal{H}_i^{\text{fx}}$ instead of $\mathcal{H}_i^{\text{fl}}$ is that $E^{(m)}$ will automatically be a valid conditional E-variable for $\mathcal{H}_0^{\text{fl}}$ and even $\mathcal{H}_0^{\text{pd}}$, as well. This is guaranteed by the following:

Lemma 4.1. *The map $E^{(m)}$ defined in 6 constitutes a conditional E-variable w.r.t. all three, $\mathcal{H}_0^{\text{pd}}$, $\mathcal{H}_0^{\text{fx}}$ and $\mathcal{H}_0^{\text{fl}}$.*

5 Classifier Two-Sample Tests with E-Variables

Here we will formalize the classifier two-sample test with E-variables. Assume that we are given two independent samples from two possibly different distributions

$$X_1^{(0)}, \dots, X_{N_0}^{(0)} \stackrel{\text{i.i.d.}}{\sim} P_0, \quad X_1^{(1)}, \dots, X_{N_1}^{(1)} \stackrel{\text{i.i.d.}}{\sim} P_1.$$

Based on these samples we want to test if those distributions are equal or not:

$$H_0 : P_0 = P_1 \quad \text{vs.} \quad H_A : P_0 \neq P_1.$$

If we introduce the binary variable Y and the abbreviation:

$$P(X|Y=0) := P_0(X), \quad P(X|Y=1) := P_1(X),$$

and pool the data points $X_n^{(y)}$ via augmenting them with a Y -component: $(X_n^{(y)}, Y_n^{(y)})$ with $Y_n^{(y)} := y$, then the pooled data set can be seen as one i.i.d. sample from

$P(X, Y)$ of size $N := N_0 + N_1$ for some unknown marginal $P(Y)$. We can then reformulate the two-sample test as an independence test:

$$H_0 : X \perp\!\!\!\perp Y \quad \text{vs.} \quad H_A : X \not\perp\!\!\!\perp Y.$$

This allows us to use the E-variables from Section 4 (without any conditioning variable Z) for (conditional) independence testing. Furthermore, since Y is a binary variable we can write any Markov kernel $P(Y|X)$ as a Bernoulli distribution:

$$P_\theta(Y|X=x) = \text{Ber}(\sigma(g_\theta(x))),$$

for some parameterized measurable function g_θ and where $\sigma(t) := \frac{1}{1+\exp(-t)}$ is the logistic sigmoid-function. So our hypothesis spaces look like:

$$\begin{aligned}\mathcal{H}_0 &= \{\text{Ber}(q_\theta) \mid \theta \in \Theta_0\}, & q_\theta &\in [0, 1], \\ \mathcal{H}_A &= \{\text{Ber}(\sigma(g_\theta)) \mid \theta \in \Theta_A\} \setminus \mathcal{H}_0,\end{aligned}$$

and the m -th conditional E-variable is given by:

$$\begin{aligned}E^{(m)}(y^{(m)} | x^{(m)}, x^{(<m)}, y^{(<m)}) &= \frac{p_A(y^{(m)} | x^{(m)}, x^{(<m)}, y^{(<m)})}{p(y^{(m)} | \hat{\theta}_0(y^{(m)}))} \\ &= \prod_{n \in \mathcal{I}^{(m)}} \left(\frac{\sigma(g_{\hat{\theta}_A^{(<m)}}(x_n))}{N_1^{(m)}/N^{(m)}} \right)^{y_n} \cdot \left(\frac{1 - \sigma(g_{\hat{\theta}_A^{(<m)}}(x_n))}{N_0^{(m)}/N^{(m)}} \right)^{1-y_n}.\end{aligned} \quad (7)$$

Note that the maximum-likelihood estimator of q_θ on $y^{(m)}$ is $\hat{q}^{(m)} = N_1^{(m)}/N^{(m)}$, the frequency of points in the m -batch that are assigned to class $y = 1$. Furthermore, g_θ here is trained on $(x^{(<m)}, y^{(<m)})$ via binary classification.

6 Experiments

In this section, we propose an evaluation procedure for comparing statistical tests in terms of combined type I and type II analysis which we refer to as a *detection error trade-off*. Based on that, we compare E-C2ST with other existing approaches on synthetic, image, and real-life MRI datasets. In all our experiments, E-C2ST shows a type I error lower than the chosen significance level $\alpha = 0.05$ which is not the case for the other baselines.

6.1 Implementation

We implement **E-C2ST** according to the testing procedure proposed in the previous section. We set $M = 2$ in all experiments. We compare it to the following baselines

- **S-C2ST** (standard C2ST), is the C2ST proposed by [LPO16]. We train a binary classifier on the augmented data. The null hypothesis is that accuracy is

0.5 and the alternative is that it larger 0.5. Following [LPO16], we assume that under the null, the accuracy is normally distributed with mean 0.5 and variance $1/(2N_{te})$.

- **L-C2ST** (logits C2ST) proposed by [CC19] is a kernel based test, which again trains a binary classifier to distinguish the two classes. The null hypothesis is rejected if the difference between the classes logits average is not significant. The p -values is computed via a permutation test. We used the implementation provided by [LXL+20].
- **D-MMD** is a deep kernel based two-sample test proposed by [LXL+20]. Here, we train a neural network to maximize the statistical test power given in [LXL+20]. The reported p -values are computed by means of a permutation test. We used the implementation provided by [LXL+20].
- **ME** and **ME-resnet**. **ME** is the mean embedding test described by [CC19, JSCG16]. **ME-resnet** is the mean embedding test with features extracted from ResNet-152 [HZRS16] trained on ILSVRC [RDS+15] which we apply in the image data experiments (see Section 6.5). We optimize for the test locations on the train data. The resulting p -values are reported on the test data. We used the implementation by [JSCG16].
- **SCF** and **SCF-resnet**. Smoothed Characteristic Functions test (SCF) is also a mean embedding test by [CC19, JSCG16] with test locations optimized on the train data. **SCF-resnet** is the mean embedding test with features extracted again from ResNet-152 trained on ILSVRC which we apply in the image data experiments (see Section 6.5). We used the implementation by [JSCG16].
- **MMD-F** and **DFDA** in their unsupervised version [KKKL20]. We used these methods for the image data. First, we extract features with ResNet-152. Then we conduct the tests by means of the proposed test statistics based on maximum mean discrepancy (the MMD-F test) and its normalized version (the DFDA test).

All experiments are discussed in detail either in the main paper or in the appendix (see Section C.1 for additional information).

6.2 Training

We split the data into train and test sets with equal sizes. We fit a model on the train data, e.g. a classifier for E-C2ST, S-C2ST, and L-C2ST, and a deep kernel model for D-MMD. The chosen network architecture for each dataset

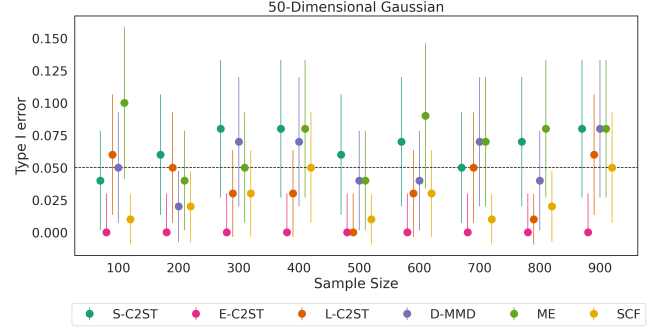


Figure 1: Estimated Type I error per method. The error bar refers to a 95% confidence interval. E-C2ST consistently has type I error lower than the significance level (dotted line) compared to the other methods.

is explained in the appendix (See Section C.1). We selected models that yield powerful two-sample tests, i.e. achieve maximum power for large enough sample sizes. To ensure a fair comparison, we fix the network architecture to be the same across models for almost all experiments. We chose a different architecture for the D-MMD method for the face expression data to increase the method’s statistical power on this task. For E-C2ST, L-C2ST and E-C2ST, we used the same trained model to perform the corresponding tests on the test data. The neural network models are trained with early stopping on a validation (20% of the train set) set to prevent overfitting. Two methods, MMD-F and DFDA, are used without training and are directly applied to the test splits for computing the corresponding test statistics.

6.3 Type-I-Error vs. Type-II-Error Trade-off

We repeat each experiment 100 times, i.e., for fixed sample size, we randomly sample a train and test set from a fixed distribution or as a subsample from a given dataset. Then, we train a model on the train set. Next, we decide whether to reject the null hypothesis with significance level $\alpha = 0.05$ on the test set. From the 100 experiments, we report the rejection rates for all methods, which corresponds to the type I error if the two classes are from the same distribution or the power ($1 - \text{type II error}$) if they are not.

We match each type II error (or equivalently, power) experiment with two type I error experiments in the following way: we first run a type II error experiment on two datasets from different distributions, followed by a type I error experiment on each of those two datasets individually. The results are summarized in *detection error trade-off* (DET) plots with type II error on the x-axes and type I error on the y-axes. The marker size depends on each class’s sample size, and the two type I error experiments are visualized with different marker styles. A test is considered to perform well if all points are below the significance level line (the dotted line) and the points approach the origin with an increasing sample size. That reflects in a test with a proper

type I error control, with converging type II error towards zero. In all experiments, only E-C2ST shows this desired property consistently. The other tests show very good type II error performance, but often with type I error above the significance level.

6.4 Synthetic Data

High-dimensional Gaussians. We start by illustrating all methods’ type I error control on a simple example. For this experiment, the two datasets are sampled from the same multivariate Gaussian distribution. We fix the dimension to be 50. Figure 1 shows the estimated type I error, i.e. the rejection rate. The error bars are the estimated 95% confidence intervals (Wald intervals) from the 100 runs. Our method consistently shows the lowest type I error, while the baseline methods often show type I error even above the significance level (visualized by the dotted line). Another method with good type I error control is SCF.

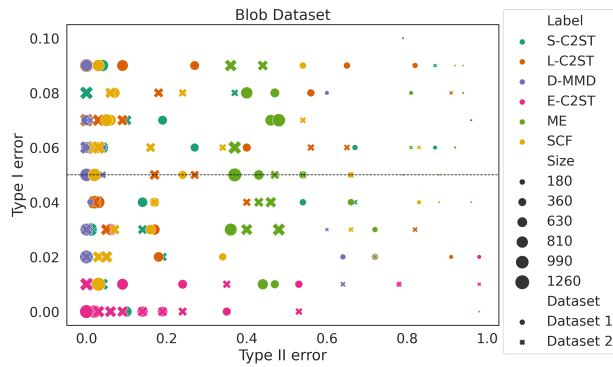


Figure 2: Detection error trade-off plot for the Blob dataset. Compared to all baselines, E-C2ST shows lower type I error than α (dotted line).

Blob Dataset. This dataset is a two-dimensional Gaussian mixture model with nine modes arranged on a 3×3 grid used by [CRSG15, GBR⁺12] in their analysis. The two distributions differ in their variance as visualized in Figure 6 in Section C.1. We carry out type I and type II error experiments as explained in Section 6.3 and display the results in a DET plot (see Figure 2). D-MMD outperforms the other methods in terms of power, at the cost of a high type I error. ME, SCF, S-C2ST, and L-C2ST often have type I error above the significance level. In contrast, E-C2ST (this paper) keeps type I error substantially below the significance level, while, as expected, the type II error decreases with increasing sample size.

6.5 Image Data

MNIST vs DCGAN-MNIST. The MNIST dataset [LBBH98] consists of 70 000 handwritten digits. As in [LXL⁺20], we compare MNIST with generated MNIST

images from a pretrained DCGAN model [RMC15]. Figure 3 makes a one-to-one comparison between our method and each baseline method. Almost all baseline methods achieve maximum power with very few samples on this task. However, we see the same tendency as before for almost all baseline methods: the estimated type I error is often higher than the significance level. An exception here is D-MMD which achieves good type I error control at the cost of power, on which it underperforms E-C2ST.

Facial Expressions. The Karolinska Directed Emotional Faces (KDEF) data set [LFÖ98] is used by [JSCG16, LPO16, KKKL20] to distinguish between positive (happy, neutral, surprised) and negative (afraid, angry, disgusted) emotions from faces. We compare all methods on the same task. As before, we compare type I vs. type II error in Figure 4. Compared to other cases, S-C2ST, D-MMD, MMD-F and DFDA have a better type I error but still higher than the one of E-C2ST. Here, ME-ResNet and SCF-ResNet do not perform well. ME-ResNet was not included in Figure 4 due to the poor results. See Section C.1 for more details.

6.6 Meta-Analysis on MRI Data

In scientific meta-analysis, outcomes from multiple studies are combined into a single conclusion. In this section, we present an experiment showing that such meta-analysis on C2STs may easily be done using E-values. In particular, following Lemma 2.2, we perform a combined test by taking the product of the three independent E-values. We combine E-values from three independent experiments of the same sample size – making a single accept/reject decision as a result of the three experiments whose data sampled from the same distributions – and show that this increases the power of E-C2ST. We compare to a meta-analysis performed with S-C2ST and L-C2ST, where we use Fisher’s method to compute combined p -values [Fis25].

For our analysis we leverage the NYU fastMRI open database containing a large number of MRI knee volumes (made up of individual slices) [ZKS⁺18], augmented with per-slice clinical pathology annotations by [ZYZ⁺22]. We restrict ourselves to the singlecoil (non-parallel imaging) setting for simplicity. As in the previous section, our experiments analyse both the type-I and type II errors. For the latter, the goal will be for a classifier to distinguish knee slices containing one or more pathologies (i.e. unhealthy) from healthy slices. To ensure independence, we partition the dataset into three equally sized parts. For each of these parts we individually train a binary classifier – consisting of the standard 16-channel fastMRI U-Net encoder [ZKS⁺18] and a single linear layer – to classify individual MRI slices. We compute E-values and p -values on the test data for each of these classifiers. We perform this procedure 100 times, and compute type I and type II errors from the resulting decisions. We refer to Appendix C.5.1 for additional details.

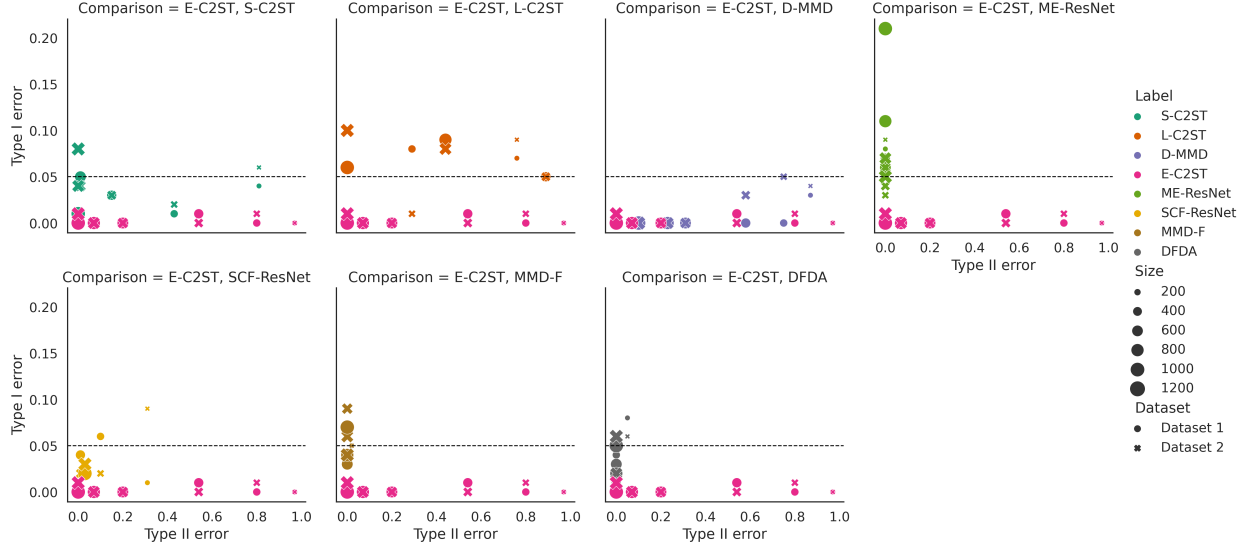


Figure 3: Detection error trade-off plots for MNIST. We compare E-C2ST to each baseline separately. E-C2ST has substantially lower type I error compared to all other methods. D-MMD also shows very good type I error control but it underperforms our method in terms of type II error.

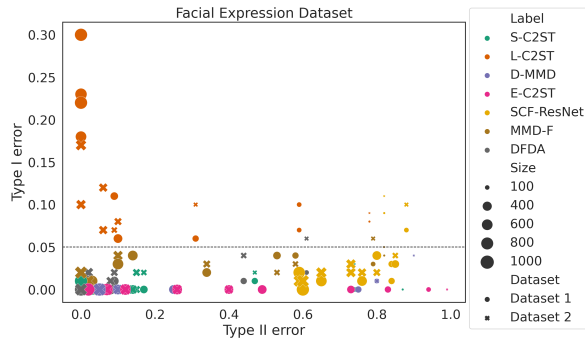


Figure 4: Detection error trade-off plot for the KDEF data for sample size = 100, 200, ..., 1000. Here most of the methods (except L-C2ST and SCF) show type I error below the significance level. E-C2ST is the only test with zero type I error.

Results are presented in Figure 5 for various sample sizes. We compare the meta-analysis using combined E-values to an analysis using the individual E-values instead (i.e. performing the statistical test on the basis of values from the three experiments individually, rather than on their combination). We also compare to similar analyses performed with S-C2ST and L-C2ST, using the same trained classifier in each case. As expected, E-C2ST dominates S-C2ST and L-C2ST on type I error for all sample sizes. Power is again lower than for the p -value tests, but is improved both by increasing sample size (as we saw for various datasets in previous experiments, and show in Appendix C.5.2 for MRI data) and by using a combination of the three independent E-values. Performing tests using the product of E-values increases power effectively, while still maintaining low type I error. Using the Fisher combination further increases the power of the p -value tests, but often at the cost of type I error, especially for L-C2ST: in some cases,

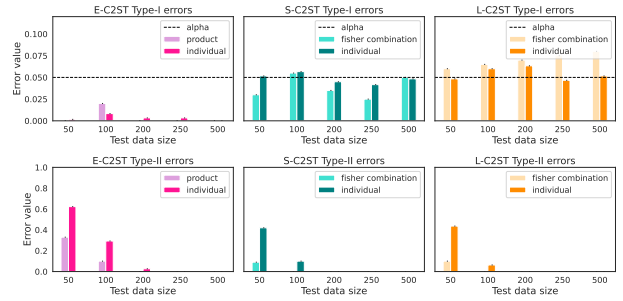


Figure 5: Meta-analysis (3 experiments) for MRI data. Testing using combined E-values increases power, while maintaining type I error control.

using the combined test statistic raises type I error above the significance threshold.

7 Conclusion

We propose E-CS2T, an E-value-based classifier two-sample test. E-CS2T combines existing frameworks on predictive conditional independence tests and split-likelihood ratio tests for constructing a valid conditional E-variable. We prove that the resulting E-variable has a finite sample type I error control. Moreover, we have empirically shown that compared to the baseline methods, E-CS2T has better type I control. However, a shortcoming of E-CS2T is that it needs to gather more evidence for correctly rejecting the null. To explore this type-I-type-II error trade-off for each statistical test, we visually combined the test's type I and type II error trajectories. Finally, we have shown on MRI data that E-variables can be utilized for combining independently conducted studies, resulting in increased power while maintaining finite sample type I error guarantees.

Acknowledgements

We would like to thank Peter Grünwald for his exciting talk at the AI4Science Colloquium, which introduced us to the theory and background of E-variables and safe testing. He inspired us to learn more about these topics and to pursue this research project.

Tim Bakker is partially supported by the **Efficient Deep Learning** research program, which is financed by the Dutch Research Council (NWO) in the domain “Applied and Engineering Sciences” (TTW).

References

- [Bal20] Akshay Balsubramani, *Sharp finite-sample concentration of independent variables*, arXiv preprint arXiv:2008.13293 (2020).
- [BBJ⁺18] Daniel J Benjamin, James O Berger, Magnus Johannesson, Brian A Nosek, E-J Wagenmakers, Richard Berk, Kenneth A Bollen, Björn Brembs, Lawrence Brown, Colin Camerer, et al., *Redefine statistical significance*, Nature human behaviour (2018).
- [BK17] Samuel Burkart and Franz J. Király, *Predictive Independence Testing, Predictive Conditional Independence Testing, and Predictive Graphical Modelling*, arXiv preprint (2017).
- [BMRS⁺22] T. Bakker, M. Muckley, A. Romero-Soriano, M. Drozdal, and L. Pineda, *On learning adaptive acquisition policies for undersampled multi-coil MRI reconstruction*, Proceedings of Machine Learning Research, 2022.
- [BvHW20] Tim Bakker, Herke van Hoof, and Max Welling, *Experimental design for MRI by greedy policy search*, Advances in Neural Information Processing Systems, 2020.
- [CC19] Xiuyuan Cheng and Alexander Cloninger, *Classification logit two-sample testing by neural networks*, arXiv preprint (2019).
- [CRSG15] Kacper P Chwialkowski, Aaditya Ramdas, Dino Sejdinovic, and Arthur Gretton, *Fast two-sample testing with analytic representations of probability measures*, Advances in Neural Information Processing Systems (2015).
- [Csi84] Imre Csiszár, *Sanov Property, Generalized I-Projection and a Conditional Limit Theorem*, The Annals of Probability (1984).
- [Fis25] R.A. Fisher, *Statistical methods for research workers*, Edinburgh Oliver & Boyd, 1925.
- [GBR⁺12] Arthur Gretton, Karsten M Borgwardt, Malte J Rasch, Bernhard Schölkopf, and Alexander Smola, *A kernel two-sample test*, The Journal of Machine Learning Research (2012).
- [GdHK20] Peter Grünwald, Rianne de Heide, and Wouter M. Koolen, *Safe Testing*, 2020 Information Theory and Applications Workshop (ITA), IEEE, 2020.
- [GH12] Michael U. Gutmann and Aapo Hyvärinen, *Noise-contrastive estimation of unnormalized statistical models, with applications to natural image statistics*, Journal of Machine Learning Research (2012).
- [GPAM⁺14] Ian Goodfellow, Jean Pouget-Abadie, Mehdi Mirza, Bing Xu, David Warde-Farley, Sherjil Ozair, Aaron Courville, and Yoshua Bengio, *Generative adversarial nets*, Advances in Neural Information Processing Systems, 2014.
- [HTF01] Trevor Hastie, Robert Tibshirani, and Jerome Friedman, *The elements of statistical learning*, Springer Series in Statistics, Springer New York Inc., New York, NY, USA, 2001.
- [HZRS16] Kaiming He, Xiangyu Zhang, Shaoqing Ren, and Jian Sun, *Deep residual learning for image recognition*, Proceedings of the IEEE conference on computer vision and pattern recognition, 2016.
- [Jr56] Kelly Jr, *A new interpretation of information rate*, World Scientific, 1956.
- [JSCG16] Wittawat Jitkrittum, Zoltán Szabó, Kacper P Chwialkowski, and Arthur Gretton, *Interpretable distribution features with maximum testing power*, Advances in Neural Information Processing Systems (2016).
- [KB14] Diederik P Kingma and Jimmy Ba, *Adam: A method for stochastic optimization*, arXiv preprint arXiv:1412.6980 (2014).
- [KKKL20] Matthias Kirchler, Shahryar Khorasani, Marius Kloft, and Christoph Lippert, *Two-sample testing using deep learning*, International Conference on Artificial Intelligence and Statistics, PMLR, 2020.
- [Kol33] Andrey Kolmogorov, *Sulla determinazione empirica di una legge di distribuzione*, Inst. Ital. Attuari, Giorn. (1933).

- [Kui60] Nicolaas H Kuiper, *Tests concerning random points on a circle*, Nederl. Akad. Wetensch. Proc. Ser. A, 1960.
- [LBBH98] Yann LeCun, Léon Bottou, Yoshua Bengio, and Patrick Haffner, *Gradient-based learning applied to document recognition*, Proceedings of the IEEE (1998).
- [LBG⁺21] Jan-Matthis Lueckmann, Jan Boelts, David Greenberg, Pedro Goncalves, and Jakob Macke, *Benchmarking simulation-based inference*, Proceedings of The 24th International Conference on Artificial Intelligence and Statistics, 2021.
- [LFÖ98] Daniel Lundqvist, Anders Flykt, and Arne Öhman, *Karolinska directed emotional faces*, Cognition and Emotion (1998).
- [LPO16] David Lopez-Paz and Maxime Oquab, *Revisiting Classifier Two-Sample Tests*, arXiv preprint (2016).
- [LXL⁺20] Feng Liu, Wenkai Xu, Jie Lu, Guangquan Zhang, Arthur Gretton, and Danica J Sutherland, *Learning deep kernels for non-parametric two-sample tests*, International conference on machine learning, PMLR, 2020.
- [MSC⁺13] Tomas Mikolov, Ilya Sutskever, Kai Chen, Greg S Corrado, and Jeff Dean, *Distributed representations of words and phrases and their compositionality*, Advances in Neural Information Processing Systems, Curran Associates, Inc., 2013.
- [MW47] Henry B Mann and Donald R Whitney, *On a test of whether one of two random variables is stochastically larger than the other*, The annals of mathematical statistics (1947).
- [PBR⁺20] Luis Pineda, Sumana Basu, Adriana Romero, Roberto Calandra, and Michal Drozdal, *Active MR k-space sampling with reinforcement learning*, International Conference on Medical Image Computing and Computer-Assisted Intervention, 2020.
- [RDS⁺15] Olga Russakovsky, Jia Deng, Hao Su, Jonathan Krause, Sanjeev Satheesh, Sean Ma, Zhiheng Huang, Andrej Karpathy, Aditya Khosla, Michael Bernstein, et al., *Imagenet large scale visual recognition challenge*, International journal of computer vision (2015).
- [RMC15] Alec Radford, Luke Metz, and Soumith Chintala, *Unsupervised representation learning with deep convolutional generative adversarial networks*, arXiv preprint (2015).
- [Sha19] Glenn Shafer, *The language of betting as a strategy for statistical and scientific communication*, arXiv preprint (2019).
- [Smi39] NV Smirnov, *Sur les hearts de la courbe de distribution empirique*, Bullentin mathdmaticque de lUniversity de Moscou. Serie international (1939).
- [SS98] Alex J Smola and Bernhard Schölkopf, *Learning with kernels*, Citeseer, 1998.
- [Stu08] Student, *The probable error of a mean*, Biometrika (1908).
- [VW21] Vladimir Vovk and Ruodu Wang, *E-values: Calibration, combination and applications*, The Annals of Statistics (2021).
- [Wel47] Bernard L Welch, *The generalization of 'student's' problem when several different population varlances are involved*, Biometrika (1947).
- [WRB20] Larry Wasserman, Aaditya Ramdas, and Sivaraman Balakrishnan, *Universal Inference*, Proceedings of the National Academy of Sciences (2020).
- [ZKS⁺18] Jure Zbontar, Florian Knoll, Anuroop Sriram, Matthew J. Muckley, Mary Bruno, Aaron Defazio, Marc Parente, Krzysztof J. Geras, Joe Katsnelson, Hersh Chandarana, Zizhao Zhang, Michal Drozdal, Adriana Romero, Michael Rabbat, Pascal Vincent, James Pinkerton, Duo Wang, Nafissa Yakubova, Erich Owens, C. Lawrence Zitnick, Michael P. Recht, Daniel K. Sodickson, and Yvonne W. Lui, *fastMRI: An open dataset and benchmarks for accelerated MRI*, CoRR (2018).
- [ZYZ⁺22] Ruiyang Zhao, Burhaneddin Yaman, Yuxin Zhang, Russell Stewart, Austin Dixon, Florian Knoll, Zhengnan Huang, Yvonne W. Lui, Michael S. Hansen, and Matthew P. Lungren, *fastMRI+, Clinical pathology annotations for knee and brain fully sampled magnetic resonance imaging data*, Scientific Data (2022).

A Type II Error Control

A general finite sample bound for the type II error of testing based on the product of (conditional) i.i.d. E-variables can be achieved by Sanov's theorem, see [Csi84, Bal20].

Theorem A.1 (Type II error control for conditional i.i.d. E-variables). *Let $E : \mathcal{X} \times \mathcal{Z} \rightarrow \mathbb{R}_{\geq 0}$ be a conditional E-variable w.r.t. \mathcal{H}_0 given \mathcal{Z} . Let $X_1, \dots, X_N : \Omega \times \mathcal{Z} \rightarrow \mathcal{X}$ be conditional random variables that are i.i.d. conditioned on \mathcal{Z} . Let $E^{(N)} := \prod_{n=1}^N E(X_n|Z)$. Let $\alpha \in (0, 1]$, $\gamma_N := -\frac{1}{N} \log \alpha \geq 0$ and for $\gamma \in \mathbb{R}_{\geq 0}$ put:*

$$\mathcal{A}_\gamma^{|z} := \{Q \in \mathcal{P}(\mathcal{X}) \mid \mathbb{E}_{X \sim Q}[\log E(X|z)] \leq \gamma\}.$$

Then for every $P_\theta \in \mathcal{H}_A$ and $z \in \mathcal{Z}$ we have the following type II error bound:

$$P_\theta \left(E^{(N)} \leq \alpha^{-1} \mid Z = z \right) \leq \exp \left(-N \cdot \text{KL}(\mathcal{A}_{\gamma_N}^{|z} \parallel P_\theta^{|z}) \right), \quad (8)$$

which converges to 0 if $\text{KL}(\mathcal{A}_{\gamma_N}^{|z} \parallel P_\theta^{|z}) > 0$ for some $\gamma > 0$. Note that for a subset $\mathcal{A} \subseteq \mathcal{P}(\mathcal{X})$ we abbreviate:

$$\text{KL}(\mathcal{A} \parallel P) := \inf_{Q \in \mathcal{A}} \text{KL}(Q \parallel P).$$

Proof. If $\hat{P}_N := \frac{1}{N} \sum_{n=1}^N \delta_{X_n|Z}$ is the empirical distribution then we get the following equivalence, when conditioned on $Z = z$:

$$\begin{aligned} E^{(N)}|z \leq \alpha^{-1} &\iff \prod_{n=1}^N E(X_n|z) \leq \alpha^{-1} \\ &\iff \frac{1}{N} \sum_{n=1}^N \log E(X_n|z) \leq -\frac{1}{N} \log \alpha =: \gamma_N \\ &\iff \mathbb{E}_{X \sim \hat{P}_N^{|z}}[\log E(X|z)] \leq \gamma_N \\ &\iff \hat{P}_N^{|z} \in \mathcal{A}_{\gamma_N}^{|z}. \end{aligned}$$

The bound then follows by a simple application of Sanov's theorem, see [Csi84, Bal20], for each $z \in \mathcal{Z}$ individually:

$$P_\theta \left(E^{(N)} \leq \alpha^{-1} \mid Z = z \right) = P_\theta \left(\hat{P}_N \in \mathcal{A}_{\gamma_N}^{|z} \mid Z = z \right) \leq \exp \left(-N \cdot \text{KL}(\mathcal{A}_{\gamma_N}^{|z} \parallel P_\theta^{|z}) \right), \quad (9)$$

which requires the i.i.d. assumption (conditioned on Z) and that $\mathcal{A}_{\gamma_N}^{|z}$ is completely convex, which it is. \square

The unconditional version follows from the above by using the one-point space $\mathcal{Z} = \{*\}$ and reads like:

Corollary A.2 (Type II error control for i.i.d. E-variables). *Let X_1, \dots, X_N be an i.i.d. sample, $E : \mathcal{X} \rightarrow \mathbb{R}_{\geq 0}$ be an E-variable w.r.t. \mathcal{H}_0 and $E^{(N)} := \prod_{n=1}^N E(X_n)$. Let $\alpha \in (0, 1]$, $\gamma_N := -\frac{1}{N} \log \alpha \geq 0$ and for $\gamma \in \mathbb{R}_{\geq 0}$ put:*

$$\mathcal{A}_\gamma := \{Q \in \mathcal{P}(\mathcal{X}) \mid \mathbb{E}_Q[\log E] \leq \gamma\}.$$

Then for every $P_\theta \in \mathcal{H}_A$ we have the following type II error bound:

$$P_\theta \left(E^{(N)} \leq \alpha^{-1} \right) \leq \exp \left(-N \cdot \text{KL}(\mathcal{A}_{\gamma_N} \parallel P_\theta) \right), \quad (10)$$

which converges to 0 if $\text{KL}(\mathcal{A}_\gamma \parallel P_\theta) > 0$ for some $\gamma > 0$.

Relating to the simpler unconditional case of the Corollary we can make the following clarifying remarks.

Remark A.3. 1. The condition: $\text{KL}(\mathcal{A}_\gamma \parallel P_\theta) > 0$ for some $\gamma > 0$, is slightly stronger than the condition: $\mathbb{E}_{P_\theta}[\log E] > 0$. If $\sup_{x \in \mathcal{X}} |\log E(x)| < \infty$ then one can show that both those conditions are equivalent.

2. If there exist $\delta, \gamma > 0$ such that for all $P_\theta \in \mathcal{H}_A$ we have $\text{KL}(\mathcal{A}_\gamma \parallel P_\theta) \geq \delta$ then we easily deduce the uniform type II error bound for $N \geq -\frac{\log \alpha}{\gamma}$:

$$\sup_{P_\theta \in \mathcal{H}_A} P_\theta \left(E^{(N)} \leq \alpha^{-1} \right) \leq \exp \left(-N \cdot \delta \right). \quad (11)$$

B Proofs

Proof of Lemma 2.2

Proof. By Fubini's theorem we get:

$$\begin{aligned}
 & \mathbb{E}_{\theta, \psi} \left[E^{(3)} \middle| z \right] \\
 &= \int E^{(3)}(x, y|z) (P_{\theta} \otimes P_{\psi}) (dx, dy|z) \\
 &= \int \int E^{(2)}(x|y, z) \cdot E^{(1)}(y|z) \\
 &\quad P_{\theta}(dx|y, z) P_{\psi}(dy|z) \\
 &= \int \left(\int E^{(2)}(x|y, z) P_{\theta}(dx|y, z) \right) \\
 &\quad \cdot E^{(1)}(y|z) P_{\psi}(dy|z) \\
 &\leq \int 1 \cdot E^{(1)}(y|z) P_{\psi}(dy|z) \leq 1. \quad \square
 \end{aligned}$$

Proof that the E-variable defined in Equation 3 is a conditional E-variable w.r.t. $\mathcal{H}_0^{(m)|(<m)}$.

Proof. For $\theta \in \Theta_0$ we have:

$$\begin{aligned}
 & \mathbb{E}_{\theta} \left[E^{(m)} \middle| x^{(<m)} \right] \\
 &= \int E^{(m)}(x^{(m)}|x^{(<m)}) p_{\theta}(x^{(m)}|x^{(<m)}) \mu(dx^{(m)}) \\
 &= \int \frac{p_A(x^{(m)}|x^{(<m)})}{\max_{\tilde{\theta} \in \Theta_0} p_{\tilde{\theta}}(x^{(m)}|x^{(<m)})} p_{\theta}(x^{(m)}|x^{(<m)}) \mu(dx^{(m)}) \\
 &\leq \int \frac{p_A(x^{(m)}|x^{(<m)})}{p_{\theta}(x^{(m)}|x^{(<m)})} p_{\theta}(x^{(m)}|x^{(<m)}) \mu(dx^{(m)}) \\
 &= \int p_A(x^{(m)}|x^{(<m)}) \mu(dx^{(m)}) = 1. \quad \square
 \end{aligned}$$

Proof of Lemma 4.1

Proof. For $\theta \in \Theta_0$ we get:

$$\begin{aligned}
 & \mathbb{E}_{\theta} \left[E^{(m)} \middle| x^{(m)}, z^{(m)}, w^{(<m)} \right] \\
 &= \int \frac{p_A(y^{(m)}|x^{(m)}, z^{(m)}, w^{(<m)})}{p(y^{(m)}|z^{(m)}, \hat{\theta}_0(y^{(m)}, z^{(m)}))} p_{\theta}(y^{(m)}|z^{(m)}) \mu(dy^{(m)}) \\
 &= \int \frac{p_A(y^{(m)}|x^{(m)}, z^{(m)}, w^{(<m)})}{\max_{\tilde{\theta} \in \Theta_0} p_{\tilde{\theta}}(y^{(m)}|z^{(m)})} p_{\theta}(y^{(m)}|z^{(m)}) \mu(dy^{(m)}) \\
 &\leq \int \frac{p_A(y^{(m)}|x^{(m)}, z^{(m)}, w^{(<m)})}{p_{\theta}(y^{(m)}|z^{(m)})} p_{\theta}(y^{(m)}|z^{(m)}) \mu(dy^{(m)}) \\
 &= \int p_A(y^{(m)}|x^{(m)}, z^{(m)}, w^{(<m)}) \mu(dy^{(m)}) = 1.
 \end{aligned}$$

This shows the claim for $\mathcal{H}_0^{\text{pd}}$. The claims for $\mathcal{H}_0^{\text{fx}}$ and $\mathcal{H}_0^{\text{fl}}$ immediately follow from Lemma 2.2 by multiplying $E^{(m)}$ with the constant E-variable 1 and $\mathcal{H}_0^{\text{pd}}$ with the hypotheses $\{P(X, Z)\}$ or $\{P_{\theta}(X, Z) \mid \theta \in \Theta_0\}$, resp. \square

Lemma B.1. *Let E_1, \dots, E_D are D E-variables with respect to the same null hypothesis class \mathcal{H}_0 . Then, the average over all D E-variables is an E-variable $\bar{E} := \frac{1}{D} \sum_{i=1}^D E_i$ is an E-variable.*

Proof. Let $p_\theta \in \mathcal{H}_0$. Then, for \bar{E} we get

$$\mathbb{E}_\theta [\bar{E}] = \int \left(\frac{1}{D} \sum_{i=1}^D E_i(x) \right) p_\theta(x) \mu(dx) = \frac{1}{D} \sum_{i=1}^D \int E_i(x) p_\theta(x) \mu(dx) \leq \frac{1}{D} \sum_{i=1}^D 1 = 1$$

□

Layer (type)	Output Shape	Param #
Linear-1	[batch size, 50]	150
BatchNorm1d-2	[batch size, 50]	100
ReLU-3	[batch size, 50]	0
Linear-4	[batch size, 50]	2550
BatchNorm1d-5	[batch size, 50]	100
ReLU-6	[batch size, 50]	0
Linear-7	[batch size, 2]	102

Table 1: The network architecture employed in the synthetic experiments for all baselines.

Layer (type)	Output Shape	Param #
Conv2d-1	[batch size, 32, 30, 30]	320
Conv2d-2	[batch size, 64, 28, 28]	18496
Dropout-3	[batch size, 64, 14, 14]	0
Linear-4	[batch size, 128] ([batch size, 600])	1605760 (7527000)
Dropout-5	[batch size, 128] ([batch size, 300])	0
Linear-6	[batch size, 2] ([batch size, 300])	258 (180300)

Table 2: The network architecture employed in the MNIST experiment for E-C2ST, L-C2ST, S-C2ST. The D-MMD architecture differences are specified in brackets.

C Experiments

In this section, we explain the implementation and training of our models in detail. In Section C.1, we discuss the architecture choice and training of E-C2ST and the other baseline methods for the synthetic and image data experiments. Additional experiments are shown in Sections C.2 and C.4. Details regarding the implementation and training of the MRI experiment are given in Sections C.5.1 and supplementary results in Section C.5.2.

C.1 Training

First, we discuss the training of the deep two-sample tests (E-C2ST, S-C2ST, L-C2ST, D-MMD). We used Adam optimizer [KB14] with learning rates $5 \cdot 1e - 4$ for the synthetic data and $1e - 4$ for the image data. The batch size for the image data is 128. For the synthetic data we used the whole dataset. In all experiments we used 80% of the training data for training and 20% for validation with early stopping.

- **High Dimensional Gaussians and Blob data.** The used network architectures are described in Table 1. For the initialization of the D-MMD parameters we used the ones provided by [LXL+20]. We trained the models with early stopping with patience 15 epochs (High Dimensional Gaussians) and 20 (50 for D-MMD) epochs (Blob data).
- **MNIST.** The dataset is obtained from <https://github.com/fengliu90/DK-for-TST>. Table 2 outlines the neural network architectures. The D-MMD architecture differs from the C2ST ones in the last two linear layer. Again we used the parameter initialization provided by [LXL+20]. We trained the models with early stopping with patience of 20 epochs.
- **Face Expression Data.** For the C2ST methods we used the DCGAN Discriminator provided in Table 3. We set the patience parameter to 10 epochs. We couldn't train D-MMD on this task by utilizing the Discriminator architecture due to the method's sensitivity to the parameter initialization. We leave this for future work. We proposed another approach inspired by [KKKL20]. We extract features by using ResNet and then we train a two-layer network with size 300 with an ReLU activation layer in-between on the extracted features with patience of 100 epochs. It yielded very good results as displayed in Figure 4.

For ME (ME-ResNet) and SCF (SCF-ResNet), we set $J = 5$ in all experiments.

C.2 High-Dimensional Gaussians.

We run E-C2ST and the other baseline methods on high-dimensional Gaussian data. For the type II error experiment, we sample the two datasets from $\mathcal{N}(0, I_{50})$ and $\mathcal{N}(0, \text{diag}(2, 1, \dots, 1))$. We run two type I error experiments on datasets either

Layer (type)	Output Shape	Param #
Conv2d-1	[batch size, 16, 16, 16]	448
LeakyReLU-2	[batch size, 16, 16, 16]	0
Dropout2d-3	[batch size, 16, 16, 16]	0
Conv2d-4	[batch size, 32, 8, 8]	4640
LeakyReLU-5	[batch size, 32, 8, 8]	0
Dropout2d-6	[batch size, 32, 8, 8]	0
BatchNorm2d-7	[batch size, 32, 8, 8]	64
Conv2d-8	[batch size, 64, 4, 4]	18496
LeakyReLU-9	[batch size, 64, 4, 4]	0
Dropout2d-10	[batch size, 64, 4, 4]	0
BatchNorm2d-11	[batch size, 64, 4, 4]	128
Conv2d-12	[batch size, 128, 2, 2]	73856
LeakyReLU-13	[batch size, 128, 2, 2]	0
Dropout2d-14	[batch size, 128, 2, 2]	0
BatchNorm2d-15	[batch size, 128, 2, 2]	256
Flatten-16	[batch size, 512]	0
Linear-17	[batch size, 100]	51300
ReLU-18	[batch size, 100]	0
Linear-19	[batch size, 2]	202

Table 3: The network architecture employed in the MNIST experiment for E-C2ST, L-C2ST, S-C2ST.

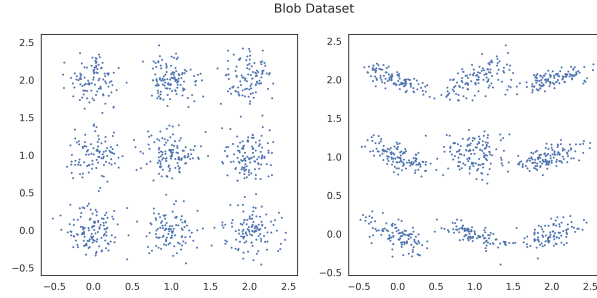


Figure 6: The two classes of the blob dataset.

sampled from $\mathcal{N}(0, I_{50})$ or $\mathcal{N}(0, \text{diag}(2, 1, \dots, 1))$, respectively. The results are displayed in Figure 9b. All methods show very good type II error control. E-C2ST has lower power in the low sample size case (sample size=100). The type I error control is above the significance level for all baseline methods but SCF. However, this method underperforms compared to the other baselines, which complies with the discussed type I and II error trade-off.

The type I error for $\mathcal{N}(0, I_{50})$ is further investigated in Section 1. We extend this experiment by increasing the sample size. Figure 7 shows the estimated type I error and the corresponding 95% confidence interval per method for sample size = 1000, 1500, 2000, 2500. Only S-C2ST shows an improvement in the type I error control compared to the results discussed in Section 1. However, both experiments do not show evidence that the methods improve their type I error control with increasing sample size.

C.3 Blob Dataset.

The two Blob distributions used in the corresponding type 2 error experiment are visualized in Figure 6. The means are the same for both classes and are arranged in a 3×3 grid. The two populations differ in their variance. Figure 9a displays the same experiment as the one in Figure 2. Here, we compare E-C2ST to one of the baseline methods in each sub-figure.

C.4 Face Expression Data

Figure 9c shows a DET plot between E-C2ST and each baseline method. This figure is another representation of the experiment from Figure 4. As we mentioned earlier, D-MMD performs as well as E-C2ST in terms of type I and type II error control. However, we used different model architectures for the training as described in Section C.1. Figure

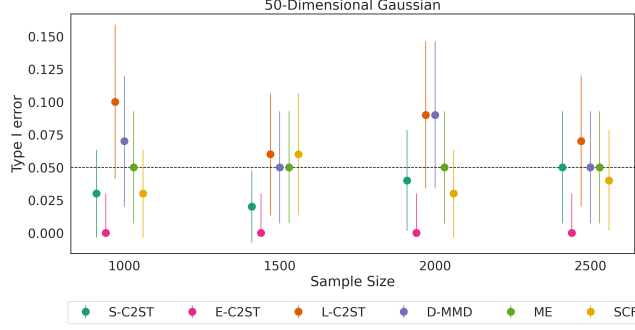


Figure 7: Type I error control. The error bars refer to 95% confidence interval. E-C2ST has the lowest type I error across all methods.

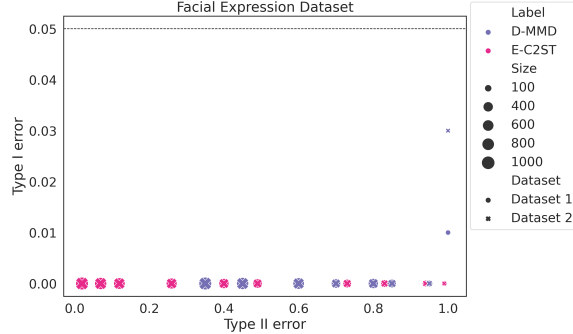


Figure 8: E-C2ST vs D-MMD. We trained D-MMD with network architecture close to E-C2ST one. The resulted D-MMD is under-powered compared to E-C2ST and with similar type I error control.

8 compares E-C2ST and D-MMD on the same task, when both models have approximately the same architecture. They differ in the last layer, where the D-MMD model has an output size of 300 as given by [LXL⁺20]. Here, D-MMD has lower power than in Figure 9c. It turns out that D-MMD performance is very sensitive to the kernel parameters initialization and we had difficulties training that model. A hyper-parameter tuning procedure is needed which we leave for future work.

C.5 MRI details

In this section we provide additional implementation details and results on the MRI data.

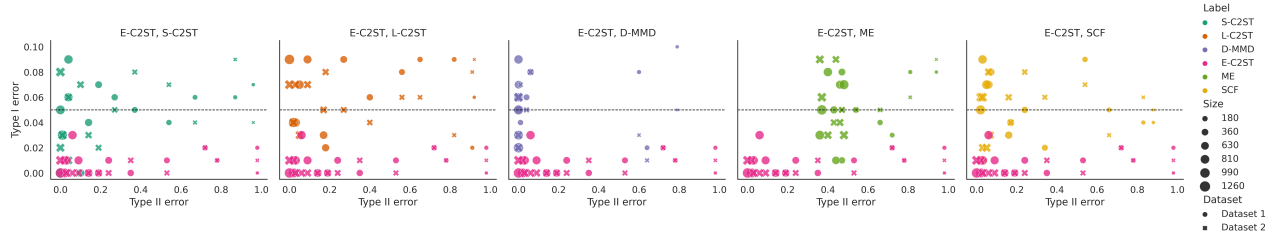
C.5.1 Data and training details

We leverage the NYU fastMRI open database containing a large number of MRI knee volumes (made up of individual slices) [ZKS⁺18], augmented with per-slice clinical pathology annotations by [ZYZ⁺22]. We restrict ourselves to the singlecoil (non-parallel imaging) setting for simplicity. We sample data from the combined fastMRI knee train and validation sets, omitting the potentially slightly differently distributed test set [PBR⁺20, BvHW20, BMRS⁺22].

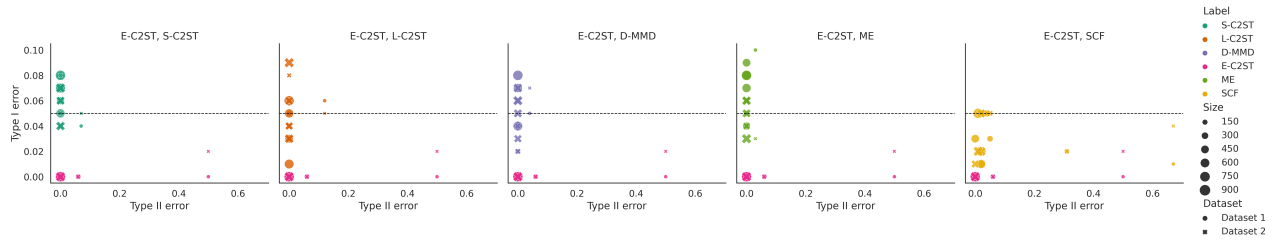
We perform our experiments on class-stratified data; since there are many more healthy than unhealthy slices in the data, we must discard some of the former. Some slices are labeled as containing no pathologies, but exist in the same volume as unhealthy slices. Since such slices are especially likely to have been mislabeled, or be correlated with nearby unhealthy slices, we discard them before stratifying the data. We call the resulting filtered dataset \mathcal{D}_f .

We then choose a dataset size N and sample $N/2$ slices of each class (healthy and unhealthy) from \mathcal{D}_f . This allows us to do two type I error tests: one for each class. For both classes, we randomly label half the data as positive and the other half as negative. We then split half the data off as test data, and split a further 20% of the remaining training data off as validation data. For the type II error tests, we instead independently sample $N/2$ slices of each class from \mathcal{D}_f , and randomly discard half, such that the total number of datapoints corresponds to the type I error experiments. Here we label the unhealthy slices as positive and the healthy ones as negative. We then perform the same train-val-test split. In each case, this results in $N/4$ test points, $N/5$ train points, and $N/20$ validation points.

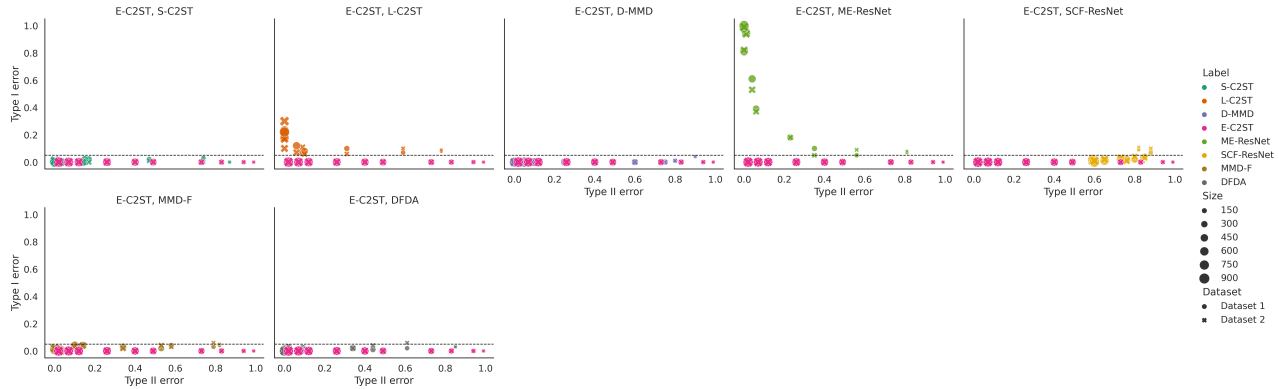
The binary classifiers – consisting of a standard 16-channel fastMRI U-Net encoder [ZKS⁺18] and a single linear layer – are trained on size 64 batches of full-resolution slices (320×320) by the Adam optimiser [KB14] with learning rate 10^{-5} .



(a) Blob Data



(b) High Dimensional Gaussians Data



(c) Face Expression Data

Figure 9: Detection error trade-off plots comparing E-C2ST and each baseline method. E-C2ST consistently shows the lowest type I error among all methods.

for 30 epochs. We employ early stopping on the validation loss with patience 3. We compute the E-value and p -value for each classifier on the test data.

C.5.2 Additional results

In this section we present two additional results: a detection error trade-off plot for MRI data similar to those shown for the other datasets in the main text, and a meta-analysis experiment using the average of E-values, following Lemma B.1.

For the detection error trade-off plot, we perform the experimental procedure outlined in Sections 6.2 and 6.3, comparing E-C2ST to S-C2ST and L-C2ST. As in Section C.4, we run into similar issues when training D-MMD. An extensive hyperparameter search is needed to find a powerful D-MMD model, which we leave for future work.

We use dataset sizes $N \in \{200, 400, 800, 1000, 2000, 3000, 4000, 5000\}$, corresponding to (test) sample sizes of 50, 100, 200, 250, 500, 750, 1000, and 1250. We repeat all experiments 100 times to compute type I and type II errors.

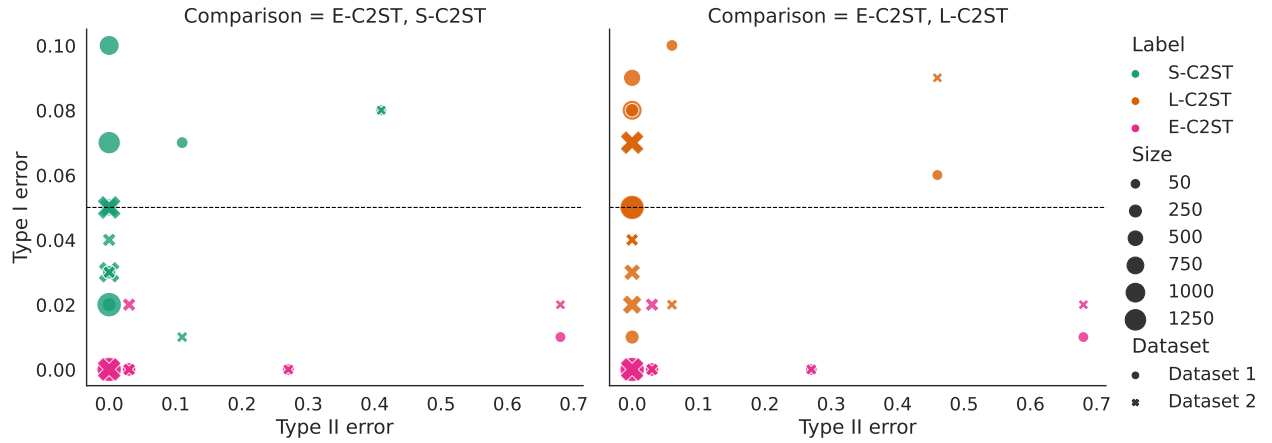


Figure 10: Detection error trade-off plot for MRI data. E-C2ST dominates S-C2ST and L-C2ST on type I error, while power converges to 1 with increased sample size.

Results are shown in Figure 10. E-C2ST shows proper type I error control across sample sizes, while S-C2ST and L-C2ST often do not achieve type I error below the significance level. Power of E-C2ST is somewhat lower than that of S-C2ST and L-C2ST for small sample sizes, but converges to 1 with more data.

In the meta-analysis experiments of the main text, we combined E-values by taking their product (Lemma 2.2) and demonstrated that this procedure improved E-C2ST’s power on MRI data while maintaining low type I error. Here we show additional results using the average of E-values (following Lemma B.1) in Figure 11. Performing tests using either the average or the product of E-values increases power effectively, while still maintaining low type I error.

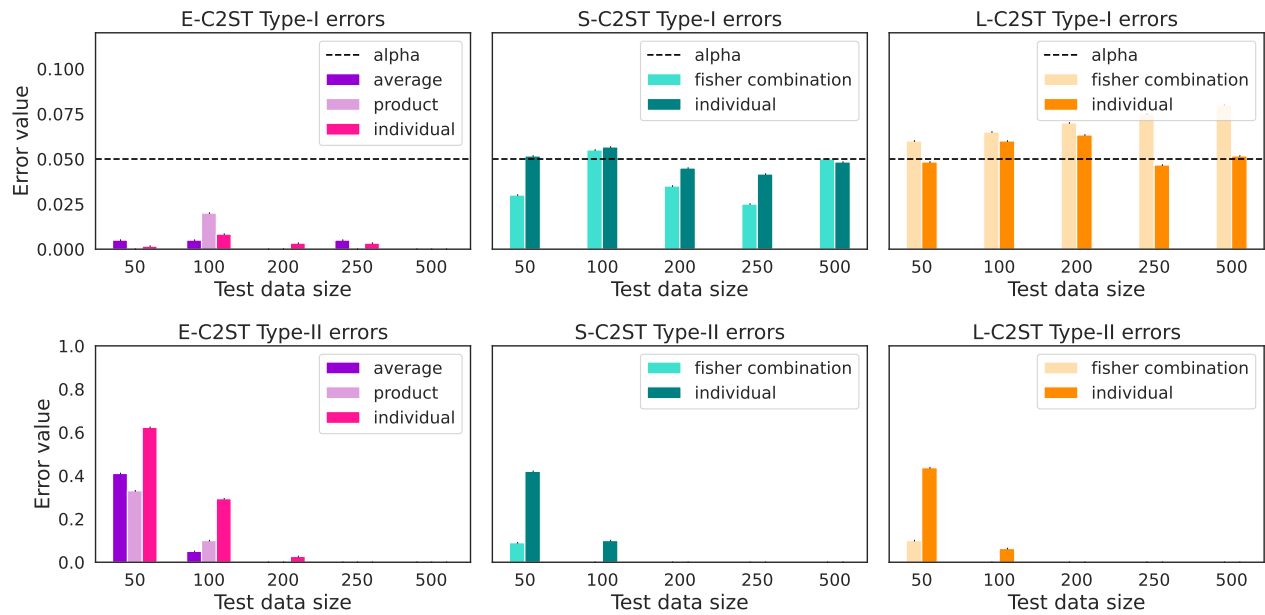


Figure 11: Meta-analysis (3 experiments) for MRI data. Testing using combined E-values increases power, while maintaining type I error control.